Supporting Information

Alyahya *et al.* 10.1073/pnas.0810794106

SI Text

SI Results

We also wanted to examine whether the *B. subtilis* RodZ homolog (formerly YmfM) plays a role in cell shape determination in this gram-positive bacterium. Repeated attempts at generating a deletion or depletion strain were unsuccessful, possibly because of a polar effect on the adjacent essential gene *pgsA*, although driving *pgsA* expression from an independent, IPTG-inducible promoter did not appear to solve the problem. Because over-production of RodZ affects cell shape in both *C. crescentus* and *E. coli*, we examined whether over-production of $RodZ_{Bs}$ from a multicopy plasmid carrying $rodZ_{Bs}$ under a xylose-inducible promoter (CJW2929; MB24/pMK3PxylA-$rodZ_{Bs}$) can cause morphological defects in *B. subtilis*. While growth in LB appeared normal (not shown), growth was inhibited in minimal medium (MM) unless magnesium and sucrose or magnesium alone were present [supporting information (SI) Fig. S6*A*]. Magnesium is commonly used to suppress cell shape defects, such as those caused by absence of MreB (1), in *B. subtilis*. Removal of magnesium in MM resulted in progressive cell widening and midcell bulging, while having no effect on a strain bearing an empty vector (AH2654; MB24/pMK3) (Fig. S6*B*).

SI Materials and Methods

Bioinformatic Analyses. Orthologs of genes of interest were identified in STRING 7.1 database (2) based on the Clusters of Orthologous Groups (COG) method (3, 4). This was complemented with a BLAST search using RodZ and MreD from *C. crescentus* as queries. Hits with e-values less than 0.1 were considered RodZ or MreD homologs. Several MreB and MreC hits were checked manually with BLAST. Specifically, *X. oryzae* has an MreC homolog not identified by STRING, and the MreB homolog identified by STRING in *M. florum* is in fact a spurious hit to an Hsp70 chaperone gene. Among the 143 RodZ sequences identified, 121 were identified by STRING and the remaining 22 by BLAST.

Multiple sequence alignment of RodZ homologs was achieved using MUSCLE 3.6 (5). The locations of TM regions were predicted using Phobius (6). For visualization of conserved domains, positions with gaps in more than 75% of sequences were removed from the alignment, and the alignment was manually edited to position properly the TM regions of proteins that lack C-terminal domains. Two sequences from the *Rickettsia* genus (315456.RF_1212 and 272947.RP757) were removed because they lacked both TM and C-terminal domains.

Because the RodZ C-terminal domain is conserved but not identified in domain databases, we used the HMMer 2.3.2 software (7) to build a hidden Markov model and scanned all protein sequences in STRING 7.1 for proteins containing the domain. The HMM was built from positions 566 to 687 of the full gapped alignment, corresponding to residues 266 to 339 of RodZ from *C. crescentus* and residues 255 to 329 of RodZ from *E. coli K12*. We found 121 matching proteins using an e-value threshold of 1e-6 in the HMMer program hmmpfam. All of those are RodZ proteins, although 5 of them were not among the 143 RodZ sequences obtained by the STRING COG and BLAST methods described above because they did not meet our set BLAST e-value threshold. The N- and C-terminal linkers are in positions 147 to 237 and 271 to 565, respectively, of the full RodZ alignment. The length of these linkers in each RodZ sequence was determined by counting the number of nongap residues in those regions of the alignment.

The phylogenetic tree was generated using MEGA 4.0 software (8), and annotated using custom Perl scripts and the GD graphics library. The input tree file was the phylogenetic tree of species in STRING 7.1, edited to leave 1 branch for the representative strain from each species group and to remove nonbacterial subtrees.

Plasmid Construction. ***pBAD18gfp-rodZ$_{Ec}$.*** *gfp-rodZ$_{Ec}$*fragment was obtained by digesting pBAD33gfp-rodZ_{Ec} with KpnI/HindIII. pBAD18 was digested similarly with KpnI/HindIII and ligated with *gfp-rodZ$_{Ec}$*. The insert was verified by sequencing.

pBAD33gfp-rodZ$_{Ec}$. *rodZ$_{Ec}$* was amplified using rodZFBamHI (ATATggatccAAATTAAGAATTAAAATGAATACTGAAGCCACGCAC) and (rodZRHindIII ATATaagcttTTACTGCGCCGGTGATTGTTC). Monomeric *gfp (mgfp)* was amplified from pKS(mYFPmcs)mGFP with primers KpnISDGFPF (GGTACCAATAAGGAGGATTTACATatggtgagcaagggcgagga) containing the *E. coli* Shine-Dalgarno sequence (AGGAGG) and GFPendBamHI (atattaGGATCCGGATTTTGTTTTGCActtgtacagctcgtccatgccg). pBAD33 was digested with KpnI and HindIII restriction enzymes. The fragments were triple ligated into pBAD33 and the insert was verified by sequencing.

pHL23Pxylgfp-rodZ. *rodZ* was amplified using BamHIFrodZ (ATATggatccAAATTAAGAATTAAACCGCTGGATACGGGGAACGT) and (HindIIIRrodZ ATATaagcttTTAGCGCGCGTTCGGCGCCGCCG). pHL23PxylCreS (courtesy of M. Cabeen) was digested with NdeI/HindIII to remove *creS*. The pHL23Pxyl backbone was gel purified to be used in the subsequent ligation reaction. *mgfp* was amplified from pKS(mYFPmcs)mGFP using GFPstartNdeI (atagctCATATGgtgagcaagggcgaggagctgtt) and GFPendBamHI (atattaGGATCCGGATTTTGTTTTGCActtgtacagctcgtccatgccg). A triple ligation reaction was carried out between the *gfp* and *rodZ* inserts into the pHL23Pxyl vector. The insert verified by sequencing.

pHL32Pxylyfp-rodZ$_{1-201}$. The pHL32 plasmid was digested with HindIII/EcoRI. A *Pxyl-yfp* fragment was gel purified upon digesting pXYFPN-5 with HindIII/KpnI. The DNA sequence corresponding to the first 201 aa of RodZ was amplified using KpnIstartrodZ (ggtaccATGCCGCTGGATACGGGGAAC) and (EcoRIfirst201jabArev CTCTgaattcTCAGGGTTCGGGCGTGGTCGAC). A triple ligation reaction was carried out by ligating *Pxyl-yfp* and *rodZ* into pHL32. The insert was verified by sequencing.

pJS14PxylrodZ. *rodZ* was amplified using primers NdeIFrodZ (ATATcatatgATGCCGCTGGATACGGGGAACG) and SpeIRrodZ (ATATactagtTTAGCGCGCGTTCGGCGCCGCC). *Pxyl* was digested from pRW432 using NdeI/EcoRI restriction enzymes. Fragments were triple ligated into pJS14 digested with SpeI/EcoRI. The orientation of *Pxyl-rodZ* was found to be against *Plac* present on the pJS14. The insert sequence was correct except for a silent mutation at codon 34 in *rodZ* where a GGC was mutated to GGT resulting in the same glycine amino acid.

pJS14Pxylcfp-rodZ. *cfp-rodZ* was obtained from pXCFPN-1rodZ by digesting the plasmid using NdeI/EcoRI enzymes and gel purifying the 1.7kb band. pJS14 was digested with NdeI/EcoRI and ligated with *cfp-rodZ*. The correct insert was verified by sequencing.

pMK3PxylA-rodZ$_{Bs}$. *PxylA* was PCR amplified using primers PxylA-266F (GACAaagcttTGATCAGCGATATCCACTTC) and

Pxyl-ymfMr (CTTGGAGATCATCCAATGACATGTGATTTCCCCCTTAAAAATAAATTC), and primers set ymfM + 1F (ATGTCATTGGATGATCTCCAAG)/ymfM+stopR (GAGgaattcATCGCGCACTCAAATCCAGGAGCTG) were used to amplify $rodZ_{Bs}$ coding sequence (previously referred as *ymfM*). A *PxylA-rodZ*$_{Bs}$ transcriptional fusion was obtained by overlapping PCR with primers PxylA-266F and ymfM+stopR using *PxylA* and $rodZ_{Bs}$ fragments as templates, and then digested with HindIII and EcoRI and cloned between the same sites of the multicopy number plasmid pMK3 (8).

pMR20PxylrodZ. pMR20 was digested with EcoRI/SpeI. *Pxyl* was obtained by digesting pRW432 with NdeI/EcoRI. *rodZ* was amplified using primers NdeIFrodZ (ATATcatatgATGCCGCTGGATACGGGGAACG) and SpeIRrodZ (ATATactagtTTAGCGCGCGTTCGGCGCCGCC). *Pxyl* and *rodZ* fragments were triple ligated into pMR20 and the sequence of the insert was verified by sequencing.

pNPTS138USΩDSrodZ. To create a *rodZ* deletion construct, 809bp of upstream *rodZ* region was amplified with primers P1 (ATGCACTAGTCGGCCCTGCTGCGCATGCAGAT) and P3 (ATATGAATTCTTGATGACCCTCTCCGCCGCCTCA) containing SpeI and EcoRI restrictions sites, respectively. The downstream *rodZ* region was amplified using primers P2 (ATGTGAATTCGTTCCCCGTATCCAGCGGCATAA) with an EcoRI site and P4 (GCTAGTCGACGATGCCGATGGCGCTCTTGAC) containing a SalI restriction site. These PCR products were digested with the respective enzymes and triple ligated into pNPTS138 digested with SalI and SpeI. The inserts were verified at this stage by sequencing. An Ω cassette carrying spectinomycin/streptomycin resistance was obtained by digesting pBOR with EcoRI and gel purifying a 2.2kb band. The Ω cassette was then ligated into EcoRI-digested pNPTS138USDS. The inserts were verified by sequencing.

pNPTS138UScfp-rodZ. 744 bp upstream of *rodZ* containing the promoter region was amplified by PCR using US rodZSpeIF (ATATactagtAACGGTCGGCCGCTGCGGATCAT) and (USrodZNdeIR ATATcatatgAATCGGCTAAACGCCCCCGAA). *cfp-rodZ* was gel purified from digestion of pXCFPN-1rodZ using NdeI/EcoRI enzymes. Following digestion of pNPTS138 with SpeI/EcoRI, *cfp-rodZ* and the 744bp region were triple ligated into pNPTS138, electroporated into DH5α. The insert was verified by sequencing.

pXCFPN-1rodZ. *rodZ* was amplified using KpnIstartrodZ (ggtaccATGCCGCTGGATACGGGGAAC) and EcoRI revRodZstop (gaattcTTAGCGCGCGTTCGGCGCCGCCG). pXCFPN-1 was digested with KpnI/EcoRI, and *rodZ* digested with the same enzyme pair was ligated into the plasmid. The insert was verified by sequencing.

pXGFPN-2rodZ. *rodZ* was amplified using KpnIstartrodZ (ggtaccATGCCGCTGGATACGGGGAAC) and EcoRIrevRodZstop (gaattcTTAGCGCGCGTTCGGCGCCGCCG). *rodZ* digested with KpnI/EcoRI was ligated into pXGFPN-2 digested with the same enzymes. The insert was verified by sequencing.

pXGFPN-2rodZ$_{115–340}$. The sequence encoding the last 240 aa of RodZ were amplified using KpnIstartlast240rodZ (ggtaccATGCTGCGCGCCCCGGTCGGCGTGC) and EcoRIrevRodZstop (gaattcTTAGCGCGCGTTCGGCGCCGCCG). The PCR product was digested, and ligated into pXGFPN-2 digested with KpnI/EcoRI. The insert was verified by sequencing.

pXGFPN-2rodZ$_{1–201}$. The sequence corresponding to the first 201 aa of RodZ was amplified using KpnIstartrodZ (ggtaccATGCCGCTGGATACGGGGAAC) and EcoRIfirst201rodZrev (CTCTgaattcTCAGGGTTCGGGCGTGGTCGAC). Following digestion with KpnI/EcoRI, the fragment was ligated into pXGFPN-2 digested with the same enzymes. The insert was verified by sequencing.

pXrodZ. pXGFP4C-1 plasmid was digested with NdeI/HindIII to remove *gfp*. The large fragment corresponding to the vector carrying *Pxyl* was then gel purified. *rodZ* was amplified using NdeIFrodZ (ATATcatatgATGCCGCTGGATACGGGGAACG) and (HindIIIRrodZ ATATaagcttTTAGCGCGCGTTCGGCGCCGCCG). *rodZ*, following digestion with NdeI/HindIII, was ligated into the *Pxyl* vector. The insert was verified by sequencing.

Strain Construction. ***CJW2158.*** CB15N was electroporated with pJS14PxylrodZ.

CJW2537. A ϕCR30 phage lysate from the original transposon mutant harboring a Himar*1* insertion at the 3′ end of the *rodZ* gene was prepared and used to transduce the mutation into a clean CB15N background.

CJW2745. Plasmid pNPTS138UScfp-rodZ was electroporated into CB15N wild-type strain. Electroporants were selected on PYE kanamycin plates. To promote a second crossover reaction, resulting in excision of the plasmid backbone and retention of the *cfp-rodZ* under the native promoter, a colony harboring the first plasmid crossover was grown and 10 μl of culture was plated on a PYE sucrose plate to select for a second recombination event. Sucrose-resistant colonies were then screened by microscopy for CFP-RodZ fluorescence.

CJW2747. pXrodZ was introduced into CB15N and the plasmid was verified to have integrated at the *xylX* locus by PCR. A ϕCR30 phage lysate carrying $\Delta rodZ$::Ω was then transduced into this strain and selected on PYE spectinomycin/streptomycin with 0.3% xylose. This strain is only viable in the presence of xylose.

CJW2748. pXGFPN-2rodZ was introduced into CB15N by electroporation. Integration of the plasmid was verified by PCR to have occurred at the *xylX* locus.

CJW2767. pXGFPN-2rodZ was mated from an S17–1 *E. coli* strain into CB15N *mreB*::*mreB*$_{Q26P}$ (CJW1715). Integration of the plasmid was verified by PCR to have occurred at the *xylX* locus.

CJW2865. pHL23Pxylgfp-rodZ was introduced into CB15N by electroporation.

CJW2866. CJW2745 was mated with S17–1 *E. coli* strain carrying pXYFP-MreB.

CJW2867. A ϕCR30 phage lysate carrying *vanA*::pMT400 (AprR) was transduced into CJW2908 containing pXCFPN-1rodZ integrated at the *xylX* locus.

CJW2868. pJS14Pxylcfp-rodZ was introduced into CB15N by electroporation.

CJW2869. pXGFPN-2rodZ$_{115–340}$ was introduced into CB15N by electroporation.

CJW2871. pBAD33gfprodZ$_{Ec}$ was introduced by electroporation into *E. coli* MC1000.

CJW2906. A ϕCR30 phage lysate carrying *vanA*::pNJH17ftsZ-mcherry (AprR) was used to transduce the construct into strain CJW2865.

CJW2907. ϕCR30 phage lysate carrying *vanA*::PVMCS-6FtsZ5′-(ChlorR)was transduced into CJW2865. This strain carries the only copy of *ftsZ* under the inducible vanillic acid promoter. Growth in the absence of vanillic acid leads to cell filamentation and eventually cell death.

CJW2908. pXCFPN-1rodZ was introduced into CB15N by electroporation.

CJW2910. A P1 lysate of *rodZ*$_{Ec}$::Kan from the original Keio deletion strain collection was made. The lysate was then used to transduce the deletion into a clean *E. coli* MC1000 background at 37 °C.

CJW2911. MC1000 cells were electroporated simultaneously with pBAD33gfprodZ$_{Ec}$ and pLE7.

CJW2912. pBAD18gfprodZ$_{Ec}$ was introduced into MC1000 cells by electroporation.

CJW2913. pBAD33gfprodZ$_{Ec}$ was transformed into *E. coli* strain PB103*mreB*<>*frt*/pFB112.

CJW2921. pXrodZ was electroporated into CB15N. Plasmid was verified to have integrated at the *xylX* locus by PCR.

CJW2923. Plasmid pNPTS138UScfp-rodZ was introduced by electroporation into CB15N.
CJW2924. Using conjugation, pMR20pXylrodZ was transferred to CJW2537.
CJW2929. The wild-type MB24 *B. subtilis* strain was transformed with the replicative multicopy vector pMK3PxylA-rodZ$_{Bs}$.
CJW2933. A ϕCR30 phage lysate carrying Δ*rodZ*::Ω (Spec/StrepR) was transduced into strain CJW2935.
CJW2934. A ϕCR30 phage lysate carrying Δ*rodZ*::Ω (Spec/StrepR) was transduced into strain CJW2936. Strain is dependent on 0.3% xylose for survival.
CJW2935. pHL32Pxylyfp-rodZ$_{1–201}$ was introduced into CB15N by electroporation. Plasmid integrated at the *xylX* locus as verified by PCR.
CJW2936. pXGFPN-2rodZ$_{1–201}$ was introduced into CB15N by electroporation. Plasmid integrated at the *xylX* locus as verified by PCR.

1. Formstone A, Errington J (2005) A magnesium-dependent mreB null mutant: implications for the role of mreB in *Bacillus subtilis*. *Mol Microbiol* 55:1646–1657.
2. von Mering C, *et al.* (2007) STRING 7-recent developments in the integration and prediction of protein interactions. *Nucleic Acids Res* 35:D358–D362.
3. Tatusov RL, Koonin EV, Lipman DJ (1997) A genomic perspective on protein families. *Science* 278:631–637.
4. Tatusov RL, *et al.* (2003) The COG database: an updated version includes eukaryotes *BMC Bioinformatics* 4:41.
5. Edgar RC (2004) MUSCLE: multiple sequence alignment with high accuracy and high throughput. *Nucleic Acids Res* 32:1792–1797.
6. Kall L, Krogh A, Sonnhammer EL (2004) A combined transmembrane topology and signal peptide prediction method. *J Mol Biol* 338:1027–1036.
7. Durbin R, Eddy S, Krogh A, Mitchison G (1998) *Biological Sequence Analysis: Probabilistic models of proteins and nucleic acids.* Cambridge University Press, Cambridge.
8. Tamura K, Dudley J, Nei M, Kumar S (2007) MEGA4: Molecular Evolutionary Genetics Analysis (MEGA) software version 4.0 *Mol Biol Evol* 24:1596–1599.

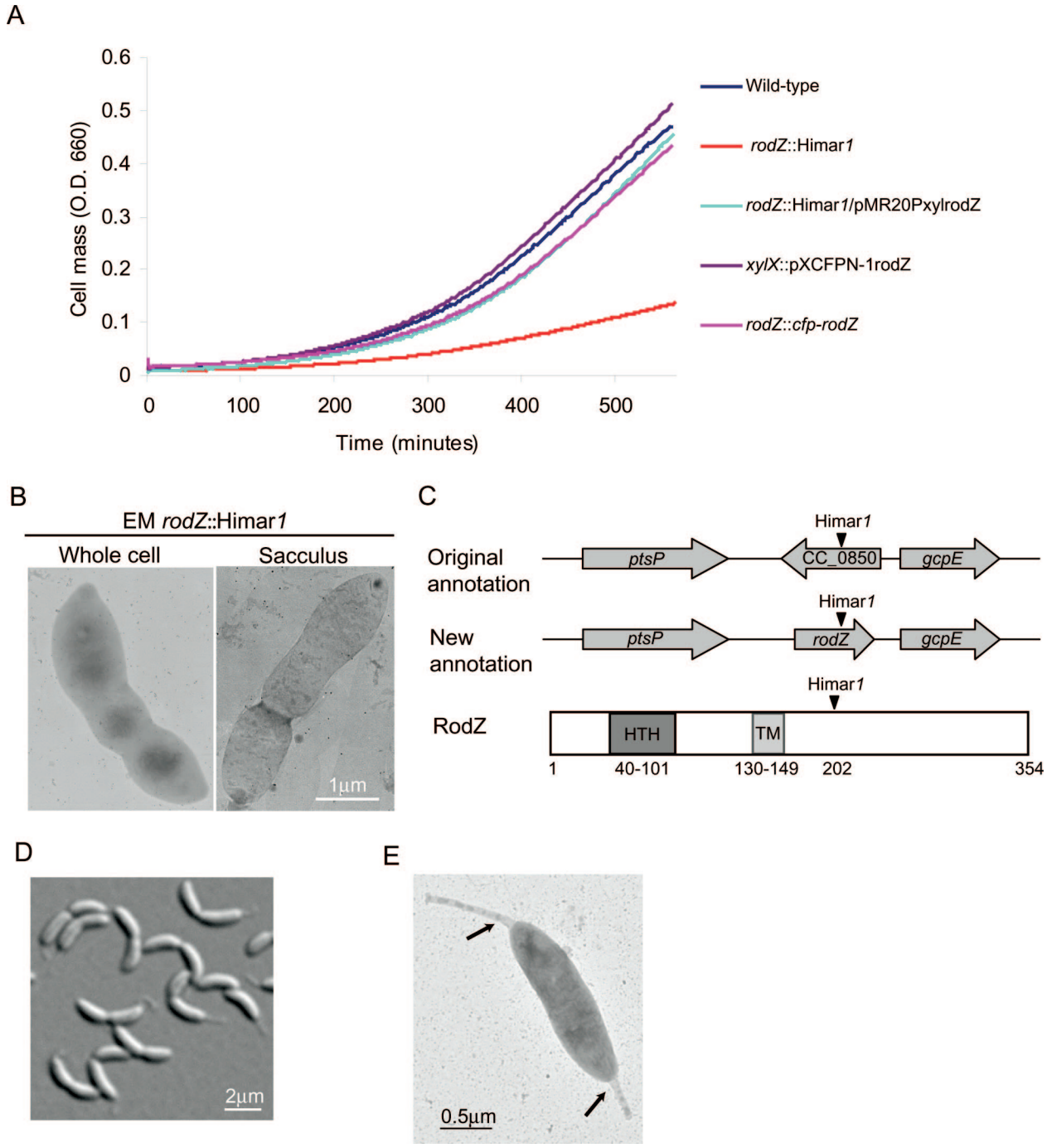

Fig. S1. RodZ plays a role in cell morphogenesis. (*A*) Optical density measurements at 660 nm were taken at 30 °C every 2 min over a period of 600 min. Strains CB15N (wild-type), CB15N *rodZ*::Himar*1* (CJW2537), and CB15N *rodZ*::*cfp-rodZ* (CJW2745) were grown in PYE. CB15N *xylX*::pXCFPN-1rodZ (CJW2908) was grown in PYE 0.3% xylose, and strain CB15N *rodZ*::Himar*1*/pMR20PxylrodZ (CJW2924) was grown in PYE 0.3% xylose + oxytetracyline (2 μg/ml). (*B*) Electron micrographs of a cell and PG sacculus of strain CB15N *rodZ*::Himar*1*. (*C*) The chromosomal region where the Himar*1* transposon inserted and the predicted domains of RodZ. (*D*) DIC micrograph of CJW2924 cells (CB15N *rodZ*::Himar*1*/pMR20PxylrodZ) grown with xylose to express *rodZ in trans*, complementing the *rodZ*::Himar*1* phenotypes. (*E*) Electron micrograph of a RodZ-overproducing cell (CJW2158; CB15N/pJS14PxylrodZ) after 10 h of xylose induction of RodZ overproduction. Black arrows denote the presence of a stalk at both ends of the cell.

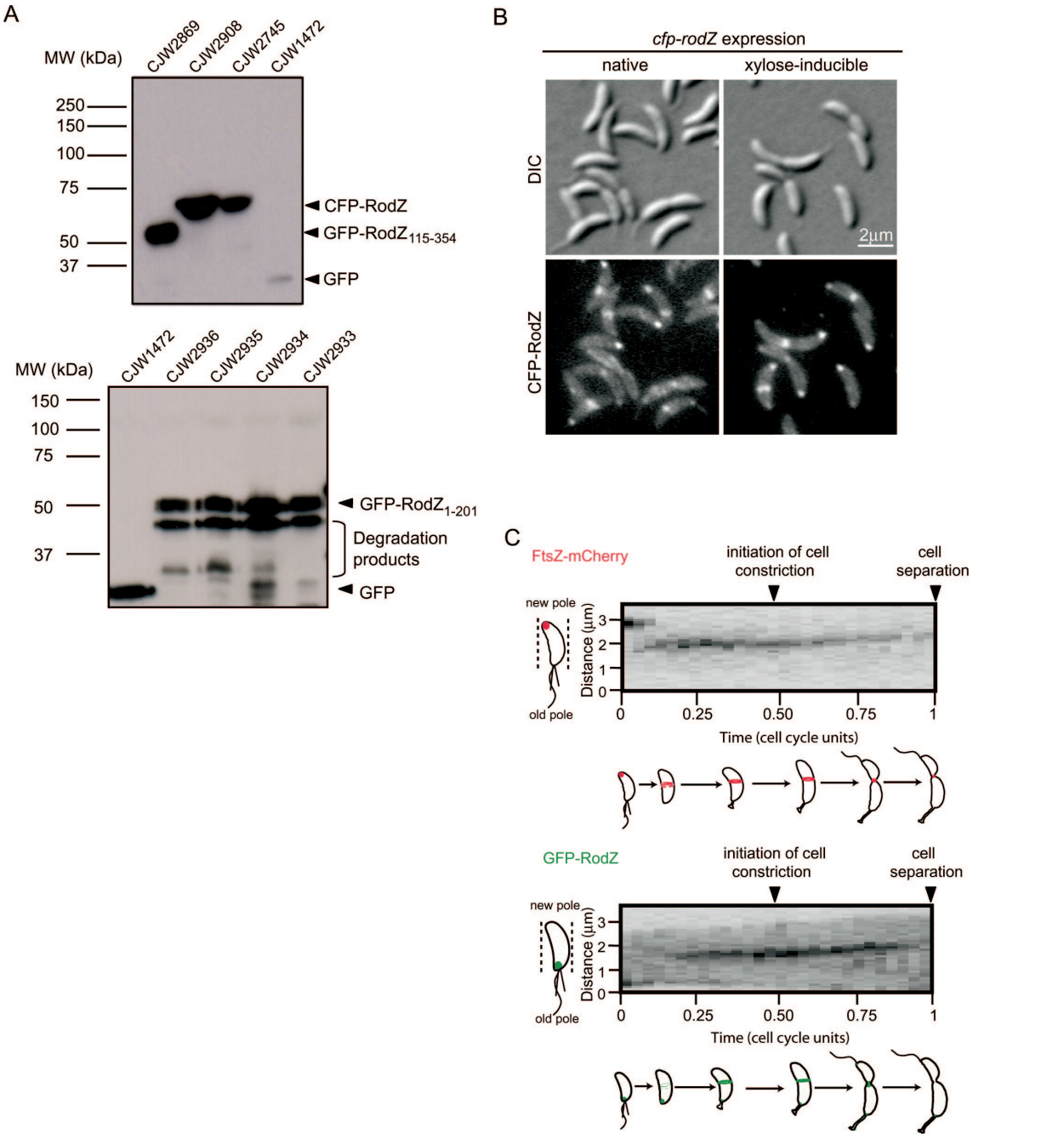

Fig. S2. RodZ accumulates near midcell shortly after FtsZ. (*A*) Western blots of RodZ fusions using anti-GFP antibodies. Cells were grown overnight, subcultured the next day in xylose for 3 h, and collected after normalizing for protein content by optical density measurements. (*Top*) Western blot, CJW2869 (CB15N *xylX*::pXGFPN-2rodZ$_{115–340}$) + xylose for 3 h to induce GFP-RodZ$_{115–340}$ synthesis; CJW2908 (CB15N *xylX*::pXCFPN-1rodZ) + xylose for 3 h to induce CFP-RodZ synthesis; CJW2745 (CB15N *rodZ*::*cfp-rodZ*) producing CFP-RodZ at native levels; CJW1472 (CB15N *xylX*::pXGFP4-C1) + xylose for 3 h to induce free GFP (used here as a control). (*Bottom*) Western blot of GFP-RodZ$_{1–201}$ showing the full-length and degradation products. Varying the linker length between GFP and RodZ$_{1–201}$ did not resolve this issue. All strains were grown in the presence of xylose for 4 h. CJW1472 (control showing migration of free GFP); CJW2936 (CB15N *xylX*::pXGPN-2rodZ$_{1–201}$); CJW2935 (CB15N *xylX*::pHL32Pxylyfp-rodZ$_{1–201}$); CJW2934 (CB15N Δ*rodZ xylX*::pXGPN-2rodZ$_{1–201}$); and CJW2933 (CB15N Δ*rodZ xylX*::pHL32Pxylyfp-rodZ$_{1–201}$). (*B*) Images of CJW2745 cells (CB15N *rodZ*::*cfp-rodZ*) or CJW2908 cells (CB15N *xylX*::pXCFPN-1rodZ) producing chromosomally encoded CFP-RodZ under native or xylose-inducible expression, respectively. For induction, xylose was added 2 h before microscopy. (*C*) Inverted kymographs depicting the maximum intensity values of FtsZ-mCherry and GFP-RodZ along the long axis of a cell for each frame. Before synchrony, CJW2906 cells (CB15N *rodZ*::pHL23Pxylgfp-rodZ *vanA*::pNJH17) were grown with xylose and vanillic acid for 2 h to preinduce expression of FtsZ-mCherry and GFP-RodZ. Swarmer cells were then placed on an agarose-padded slide containing xylose and vanillic acid, and imaged every 5 min. The new pole is oriented toward the top. Time is annotated in cell cycle units; the cell cycle is about 250 min under these conditions.

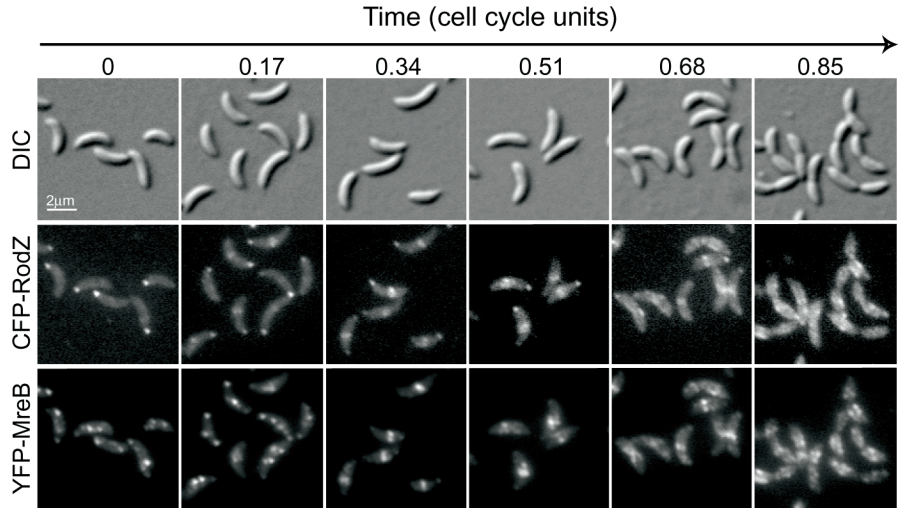

Fig. S3. RodZ localization shows temporal and spatial overlap with that of MreB. Strain CJW2866 (CB15N *rodZ*::*cfp-rodZ xylX*::pXYFP-mreB) was grown with xylose for 2 h before synchronization to induce the expression of *yfp-mreB*. Synchronized swarmer cells were resuspended in PYE with xylose and samples were taken at regular time intervals to examine the localization of YFP-MreB and CFP-RodZ over the cell cycle.

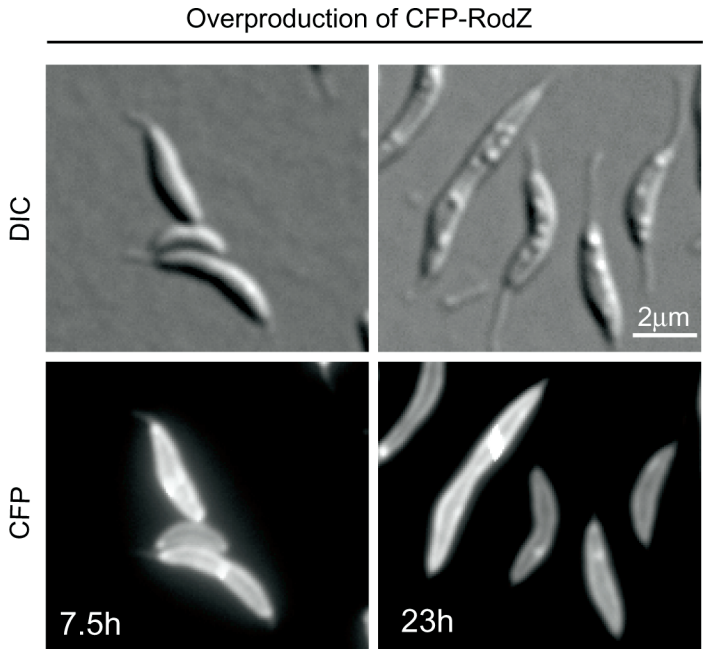

Fig. S4. Overproduction of RodZ leads to a largely diffuse membrane distribution. After growth in PYE glucose, CJW2868 cells (CB15N/pJS14Pxylcfp-rodZ) were grown in PYE xylose (to induce CFP-RodZ synthesis from *Pxyl* carried on a medium-copy plasmid) and imaged at indicated times.

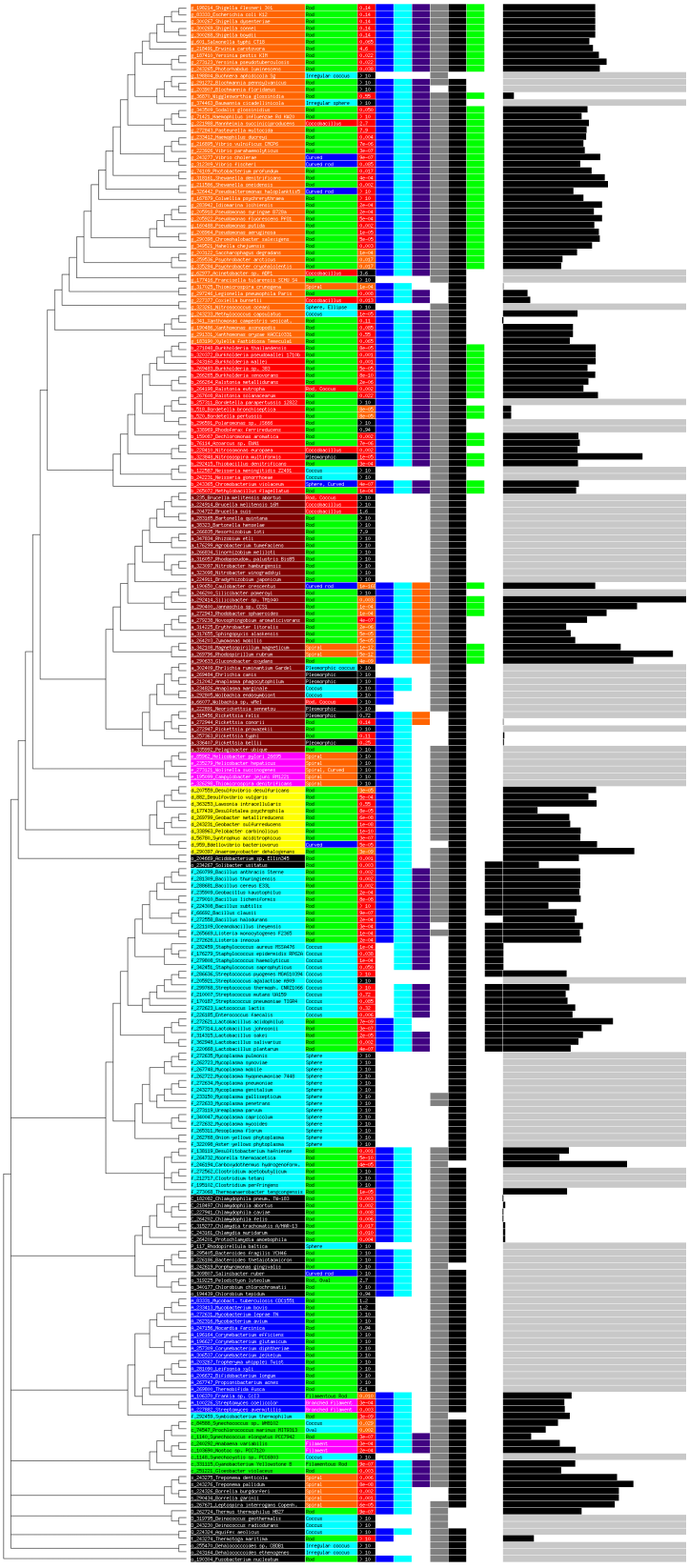

Fig. S5. Phylogenetic tree of bacterial species annotated with information pertinent to RodZ. (*Column 1*) National Center for Biotechnology Information Taxonomy ID and species name. The first character and color coding indicate phylogeny: g, orange, γ-proteobacteria; b, red, β-proteobacteria; a, maroon, α-proteobacteria; e, magenta, ε-proteobacteria; d, yellow, δ-proteobacteria; f, cyan, Firmicutes (low %GC gram-positive); A, blue, Actinobacteria (high %GC gram-positive); c, green, cyanobacteria; o, black, others, including *Chlamydia* (C), Bacteroides (B), spirochetes (s), Deinococcus (D), Aquifex (Q), and Thermotoga (t). (*Column 2*) Cell shape: rod (*green*), coccus, sphere, or oval (*cyan*); curved (*blue*); Coccobacillus (*red*); spiral (*orange*); pleomorphic (*black*); filament or branched filament (*magenta*). (*Column 3*) Presence of RodZ sequence in genome. The number indicates the lowest e-value BLAST hit against the RodZ sequence from *C. crescentus*, up to a maximum e-value of 10. Black indicates that a RodZ homolog was identified by STRING COG. Gray indicates that a RodZ homolog not identified by STRING COG was found by BLAST search with an e-value $<=$ 0.1. Red indicates that no RodZ homolog was identified by either method. (*Columns 4–8*) Presence of MreB (*blue*), MreC (*cyan*), MreD (*purple*/*orange*), GcpE (*gray*), and PgsA (*black*) proteins in the genome. In *Column 6*, purple indicates that MreD was identified by STRING, orange that MreD was identified by BLAST. (*Column 9*) A green bar indicates that *rodZ* and *gcpE* genes are adjacent on the chromosome. (*Column 10*) A black bar indicates that *rodZ* and *pgsA* genes are adjacent on the chromosome. (*Column 11*) Length of RodZ's extracellular/periplasmic region. The length was scaled to that of the longest extracellular/periplasmic region (405 residues in *Silicibacter* sp. TM1040). Genomes with no RodZ homologs have a gray bar in this column to distinguish them visually from genomes that have RodZ with a short C-terminal domain.

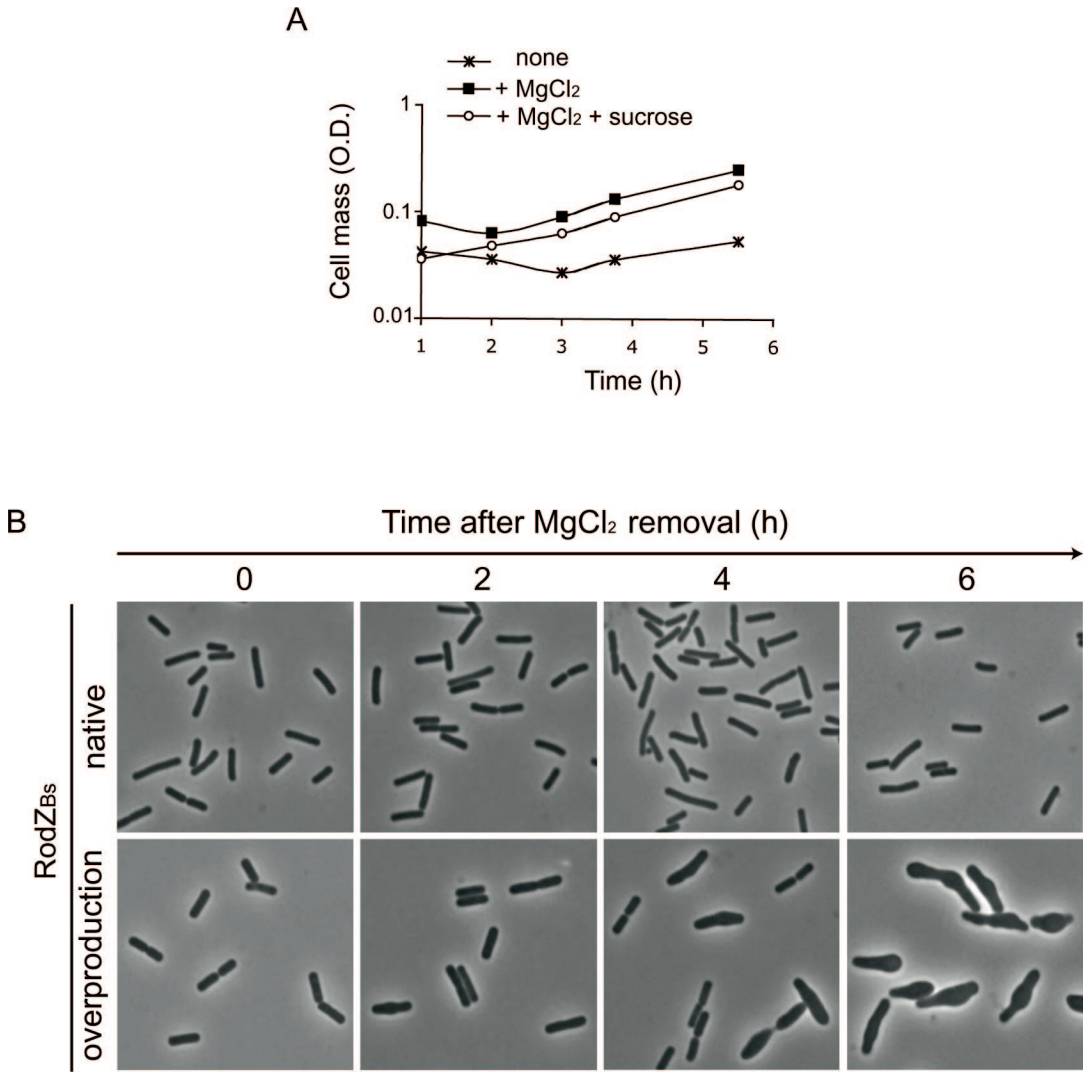

Fig. S6. Overproduction of $RodZ_{Bs}$ (formerly YmfM) leads to cell shape defects in minimal medium. (*A*) Strain CJW2929 (MB24/pMK3PxylA-$rodZ_{Bs}$) was grown in Spizizen's minimal medium (SMM; supplemented with 50-μg/ml methionine and 1-μg/ml neomycin) in the absence or presence of 20-mM $MgCl_2$ with or without 0.5M sucrose. Optical density measurements at 600 nm were taken every hour over a period of 6 h at 37 °C. (*B*) Phase contrast microscopy images of $RodZ_{Bs}$-over-producing cells were taken every 2 h over a period of 6 h after removal of $MgCl_2$. AH2654 (MB24/pMK3; control strain carrying empty vector) and CJW2929 (MB24/pMK3PxylA-$rodZ_{Bs}$) cells were grown overnight at 37 °C in SMM containing 1% xylose and 20-mM $MgCl_2$. Cells were then washed and diluted 1:10 in the same medium containing no $MgCl_2$. Images are scaled identically.

Table S1. Transduction experiments of Δ*rodZ*::Ω into various *C. crescentus* strain backgrounds

Strain	*rodZ* allele expressed from *Pxyl* at *xylX* locus	No. of Δ*rodZ*::Ω transductants
CJW27	None	0
CJW2921	*rodZ*	35+/– 3
CJW2748	*gfp-rodZ*	34+/–11
CJW2936	*gfp-rodZ*$_{1–201}$	30+/–13
CJW2869	*gfp-rodZ*$_{115–354}$	0

Equal phage ΦCR30 aliquots of transducing lysate were mixed with equal amounts of culture, incubated for 30 min at room temperature, and plated on PYE containing spectinomycin/streptomycin and xylose, and the colonies were counted after 2 days of incubation at 30°C. These are results from 3 separate experiments.

Table S2. Transduction experiments of Δ*rodZ*$_{Ec}$ into various *E.coli* strain backgrounds

Strain	Genotype	No. of colonies obtained from transducing Δ*rodZ*$_{Ec}$::*Kan* P1 lysate	
		37°C	RT
CJW1924	MC1000 (without plasmid)	20+/–15	0
CJW2871	MC1000/pBAD33*gfprodZ*$_{Ec}$ (*gfp-rodZ* expressed *in trans*)	44+/– 1	46+/–5

Results from three independent transduction experiments. Equal aliquots of culture were mixed with equal amounts of lysate. The transductants were then plated on LB-Kanamycin or LB-Kanamycin-Chloramphenicol + arabinose, and incubated at indicated temperatures for 1 day.

Table S3. Strains and plasmids used in this study

Strain or plasmid	Relevant genotype or description	Reference or source
Strains		
C. crescentus		
CJW27	CB15N (or NA1000) synchronizable variant of CB15	(1)
CJW1472	CB15N *xylX*::pXGFP4C-1	(2)
CJW1715	CB15N *mreB*::$mreB_{Q26P}$	(3)
CJW2158	CB15N/pJS14PxylrodZ	Present study
CJW2537	CB15N *rodZ*::Himar*1*	Present study
CJW2745	CB15N *rodZ*::*cfp-rodZ*	Present study
CJW2747	CB15N Δ*rodz*::Ω *xylX*::pXrodZ	Present study
CJW2748	CB15N *xylX*::pXGFPN-2rodZ	Present study
CJW2767	CB15N *mreB*::$mreB_{Q26P}$ *xylX*::pXGFPN-2rodZ	Present study
CJW2865	CB15N *rodZ*::pHL23Pxylgfp-rodZ	Present study
CJW2866	CB15N *rodZ*::*cfp-rodZ xylX*::pXYFP-mreB	Present study
CJW2867	CB15N *xylX*::pXCFPN-1rodZ *vanA*::pMT400	Present study
CJW2868	CB15N/pJS14Pxylcfp-rodZ	Present study
CJW2869	CB15N *xylX*::pXGFPN-2$rodZ_{115–340}$	Present study
CJW2906	CB15N *rodZ*::pHL23Pxylgfp-rodZ *vanA*::pNJH17	Present study
CJW2907	CB15N *rodZ*:: pHL23Pxylgfp-rodZ *ftsZ*::PVMCS-6FtsZ5′	Present study
CJW2908	CB15N *xylX*::pXCFPN-1rodZ	Present study
CJW2921	CB15N *xylX*::pXrodZ	Present study
CJW2923	CB15N *rodZ*::pNPTS138UScfp-rodZ	Present study
CJW2924	CB15N *rodZ*::Himar*1*/pMR20PxylrodZ	Present study
CJW2933	CB15N Δ*rodz*::Ω *xylX*::pHL32Pxylyfp-$rodZ_{1–201}$	Present study
CJW2934	CB15N Δ*rodz*::Ω *xylX*::pXGFPN-2$rodZ_{1–201}$	Present study
CJW2935	CB15N *xylX*::pHL32Pxylyfp-$rodZ_{1–201}$	Present study
CJW2936	CB15N *xylX*::pXGFPN-2$rodZ_{1–201}$	Present study
CJW2951	CB15N *ftsZ*::pVMCS-6FtsZ5′	Montero-Llopis P
E. coli		
CJW2871	MC1000/pBAD33 gfp$rodZ_{Ec}$	Present study
CJW2894	PB103*mreB*<>*frt*/pFB112	(4)
CJW2910	MC1000 Δ$rodz_{Ec}$::*Kan*	Present study
CJW2911	MC1000/pBAD33 gfp$rodZ_{Ec}$/pLE7	Present study
CJW2912	MC1000/pBAD18 gfp$rodZ_{Ec}$	Present study
CJW2913	PB103*mreB*<>*frt*/pFB112/pBAD33 gfp$rodZ_{Ec}$	Present study
CJW2946	MC1000 Δ$rodz_{Ec}$::*Kan*/*pLE7*	Present study
DH5α	Cloning strain	Invitrogen
K-12 BW25113	*rrnB3* DE*lacZ4787 hsdR514* DE(*araBAD*)*567* DE(*rhaBAD*)*568 rph-1*	(5)
K-12 BW25113 Δ$rodZ_{Ec}$	K-12 BW25113 Δ$rodz_{Ec}$::*Kan*	(6)
MC1000	*F- araD139* Δ *(ara,leu)7697*Δ *(lac)chi74 galU- galK- rpsL*	(7)
PB103	*dadR trpE trpA tna*	(8)
S17–1	RP4–2, *Tc*::*Mu*, *KM*-Tn*7*, for plasmid mobilization	(9)
B. subtilis		
AH2654	MB24/pMK3	(10)
CJW2929	MB24/pMK3P*xylA-*$rodZ_{Bs}$	Present study
MB24	*trpC2 metC3*	Henriques AO
Plasmids		
pBAD18	ChlorR high copy number plasmid containing *Para*	(11)
pBAD18 gfp-$rodZ_{Ec}$	pBAD18 containing a translational fusion of *gfp-*$rodZ_{Ec}$ *under Para*	Present study
pBAD33	ChlorR medium copy number plasmid containing *Para*	(11)
pBAD33 gfp-$rodZ_{Ec}$	pBAD33 containing a translational fusion of *gfp-*$rodZ_{Ec}$ *under Para*	Present study
pBOR	AmpR and Spec/StrepR pBluescriptKS + carrying Ω cassette	Stevens C
pHL23	KanR integration vector	(12)
pHL23pXyl	KanR integration vector containing a *Pxyl* followed by a multicloning site	Cabeen M
pHL23Pxylgfp-rodZ	pHL23 vector containing translational fusion of *gfp-rodZ* under *Pxyl*	Present study
pHL32	KanR integration vector	(3)
pHL32Pxylyfp-$rodZ_{1–201}$	pHL32 vector carrying translational fusion of *yfp-*$rodZ_{1–201}$ *under Pxyl*	Present study
pJS14	ChlR pBBR1-derived medium copy number broad host range vector	Skerker J

Strain or plasmid	Relevant genotype or description	Reference or source
pJS14PxylrodZ	pJS14 vector carrying *rodZ* controlled by *Pxyl*	Present study
pJS14Pxylcfp-rodZ	pJS14 vector carrying *cfp-rodZ* controlled by *Pxyl*	Present study
pBluescriptKS+	AmpR cloning vector	Stratagene
pBluescriptKS + mYFP	AmpR pBluescriptKS + carrying *myfp*	(13)
pBluescriptKS+ (mYFPmcs)mGFP	AmpR pBluescriptKS + carrying *mgfp* with the multicloning site from pBluescriptKS + mYFP	Lam H
pLE7	Medium copy AmpR plasmid containing *Plac-yfp-mreB*	(14)
pMK3	*B. subtilis* NeoR high copy number plasmid	(15)
pMK3PxylA-rodZ$_{Bs}$	pMK3 plasmid carrying *rodZ$_{Bs}$ under control of PxylA*	Present study
pMR20	OxytetR low-copy-number broad host range vector	(16)
pMR20PxylrodZ	pMR20 carrying *rodZ* controlled by *Pxyl*	Present study
pMT400	AprR integration plasmid carrying *ftsZ-yfp* under control of *Pvan*	(17)
pNJH17	AprR integration vector carrying *ftsZ-mCherry* under *Pvan*	Thanbichler M, Hillson N, and Shapiro L
pNPTS138	KanR pLitmus38-derived vector with *oriT* and *sacB*	Alley MRK
pNPTS138USΩDSrodZ	pNPTS138 vector carrying the upstream and downstream regions of *rodZ* flanking a Spec/StrepR Ω cassette	Present study
pNPTS138UScfp-rodZ	pNPTS138 vector carrying 744bp of upstream *rodZ* region and *cfp-rodZ*	Present study
pRW432	AmpR and KanR cloning vector carrying 500bp of the *Pxyl* promoter	Wright R
pVMCS-6FtsZ5′	ChlorR integrative plasmid containing the 5′region of *ftsZ under Pvan* control	Montero-Llopis P
pXCFPN-1	Spec/StrepR integration vector carrying *gfp* fusion under *Pxyl*	(18)
pXCFPN-1rodZ	pXCFPN-1 vector harboring a translational fusion of *cfp-rodZ*	Present study
pXGFP4C-1	KanR integration vector carrying *gfp* under *Pxyl*	Alley MRK
pXGFPN-2	KanR integration vector carrying *gfp* under *Pxyl*	(18)
pXGFPN-2rodZ	pXGFPN-2 vector harboring a translational fusion of *gfp-rodZ*	Present study
pXGFPN-2rodZ$_{115–340}$	pXGFPN-2 vector harboring a translational fusion of *gfp-rodZ$_{115–340}$*	Present study
pXGFPN-2rodZ$_{1–201}$	pXGFPN-2 vector harboring a translational fusion of *gfp-rodZ$_{1–201}$*	Present study
pXYFPN-5	OxytetR integration vector carrying *yfp* fusion under *Pxyl*	(18)
pXYFP-MreB	KanR pXGFP4C-1 plasmid containing *yfp-mreB* instead of *gfp* under *Pxyl*	(19)
pXrodZ	pXGFP4C-1 plasmid in which *rodZ* was inserted in place of *gfp* and is controlled by *Pxyl*	Present study

1. Evinger M, Agabian N (1977) Envelope-associated nucleoid from *Caulobacter crescentus* stalked and swarmer cells. *J Bacteriol* 132(1): 294–301
2. Costa T, Priyadarshini R, Jacobs-Wagner C (2008) Localization of PBP3 in *Caulobacter crescentus* is highly dynamic and largely relies on its functional transpeptidase domain. *Mol Microbiol.* 70:634–651.
3. Aaron M, *et al.* (2007) The tubulin homologue FtsZ contributes to cell elongation by guiding cell wall precursor synthesis in *Caulobacter crescentus*. *Mol Microbiol.* 64:938–952
4. Bendezu FO, de Boer PA (2008) Conditional lethality, division defects, membrane involution, and endocytosis in mre and mrd shape mutants of *Escherichia coli*. *J Bacteriol* 190:1792–1811
5. Datsenko KA, Wanner BL (2000) One-step inactivation of chromosomal genes in *Escherichia coli* K-12 using PCR products. *Proc Natl Acad Sci USA* 97:6640–6645
6. Baba T, *et al.* (2006) Construction of *Escherichia coli* K-12 in-frame, single-gene knockout mutants: the Keio collection. *Mol Sys Biol* 2:1–11.
7. Casadaban MJ, Cohen SN (1980) Analysis of gene control signals by DNA fusion and cloning in *Escherichia coli*. *J Mol Biol* 138:179–207
8. de Boer P, Crossley RE, Rothfield LI (1988) Isolation and properties of minB, a complex genetic locus involved in correct placement of the division site in *Escherichia coli*. *J Bacteriol* 170:2106–2112
9. Simon R, Prieffer U, Puhler A (1983) A broad range host mobilization system for *in vivo* genetic engineering: Transposon mutagenesis in gram negative bacteria. *Biotechnology* 1,784–790
10. Ozin AJ, Costa T, Henriques AO, Moran CP Jr (2001) Alternative translation initiation produces a short form of a spore coat protein in *Bacillus subtilis*. *J Bacteriol* 183:2032–2040
11. Guzman LM, Belin D, Carson MJ, Beckwith J (1995) Tight regulation, modulation, and high-level expression by vectors containing the arabinose PBAD promoter. *J Bacteriol* 177:4121–4130
12. Lam H, Schofield WB, Jacobs-Wagner C (2003) A landmark protein essential for establishing and perpetuating the polarity of a bacterial cell. *Cell* 124:1011–1023
13. Matroule JY, Lam H, Burnette D, Jacobs-Wagner C (2002) Cytokinesis monitoring during development; rapid pole-to-pole shuttling of a signaling protein by localized kinase and phosphatase in *Caulobacter*. *Cell* 118:579–590
14. Shih YL, Le T, Rothfield L (2003) Division site selection in *Escherichia coli* involves dynamic redistribution of Min proteins within coiled structures that extend between the two cell poles. *Proc Natl Acad Sci USA* 100:7865–7870
15. Sullivan AM, Yasbin RE, Young FE (1984) New shuttle vectors for *Bacillus subtilis* and *Escherichia coli* which allow rapid detection of inserted fragments. *Gene* 29(1–2):21–26
16. Roberts RC, *et al.* (1996) Identification of a *Caulobacter crescentus* operon encoding hrcA, involved in negatively regulating heat-inducible transcription, and the chaperone gene grpE. *J Bacteriol* 178:1829–1841
17. Thanbichler M, Shapiro L (2006) MipZ, a spatial regulator coordinating chromosome segregation with cell division in *Caulobacter*. *Cell* 126(1):147–162.
18. Thanbichler M, Iniesta AA, Shapiro L (2007) A comprehensive set of plasmids for vanillate- and xylose-inducible gene expression in *Caulobacter crescentus*. *Nucleic Acids Res* 35:e137.
19. Dye NA, Pincus Z, Theriot JA, Shapiro L, Gitai Z (2005) Two independent spiral structures control cell shape in Caulobacter. *Proc Natl Acad Sci USA* 102:18608–18613.